

## Electronic Supplementary Information (ESI)

### Highly selective detection of 2,4,6-trinitrophenol by using newly developed terbium-doped blue carbon dots

Bin Bin Chen<sup>a</sup>, Ze Xi Liu<sup>b</sup>, Hong Yan Zou<sup>b</sup> and Cheng Zhi Huang<sup>\*ab</sup>

<sup>a</sup> Key Laboratory of Luminescent and Real-Time Analytical Chemistry (Southwest University), Ministry of Education, College of Chemistry and Chemical Engineering, Southwest University, Chongqing 400715, China. E-mail: chengzhi@swu.edu.cn, Tel: (+86) 23 68254059, Fax: (+86) 23 68367257

<sup>b</sup> Chongqing Key Laboratory of Biomedical Analysis (Southwest University), Chongqing Science & Technology Commission, College of Pharmaceutical Science, Southwest University, Chongqing 400716, China

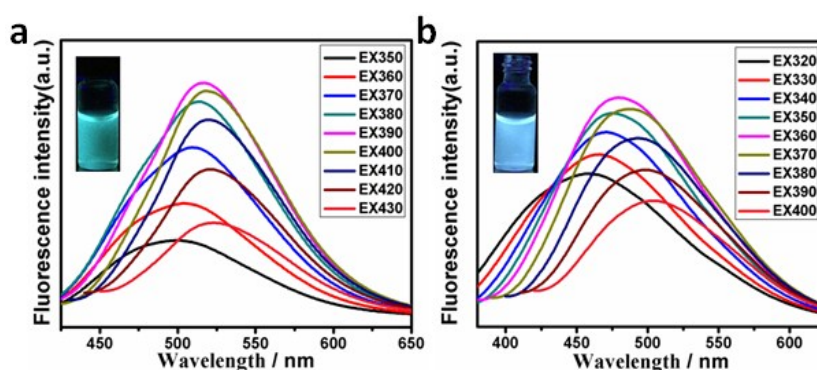


**Fig. S1** The preparation of Tb-CDs by using different Tb salts. (a)  $\text{TbCl}_3$  (Inset: Tb-CDs solution under the 365 nm UV lights lamp); (b)  $\text{Tb}_2(\text{SO}_4)_3$  (Inset: Tb-CDs solution under the 365 nm UV lights lamp).

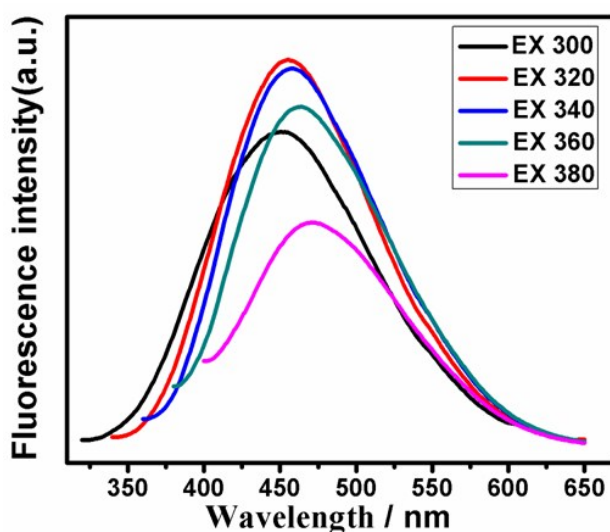


**Fig.S2** The emission spectrum of Tb-CDs.

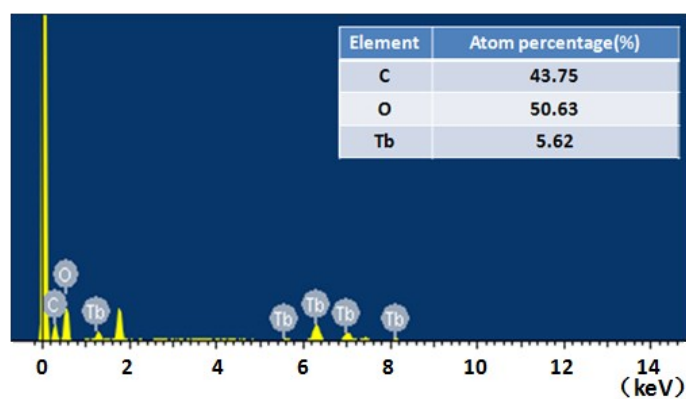


**Fig.S3** The EDX analysis of Tb-CDs.

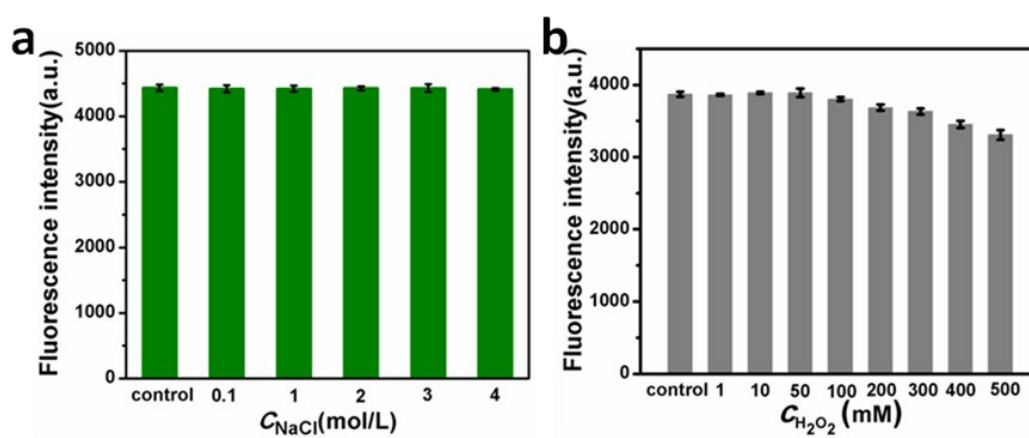


**Fig.S4** The stability investigation of the as-prepared Tb-CDs. (a) The stability in a salty medium; (b) the antioxidant capacity of Tb-CDs.  $C_{\text{Tb-CDs}}$ , 0.4 mg/ml.

**Table. S1** Zeta potentials vary from different pH value.

pH	Zeta potential (mV)
1.81	23.5
2.21	16.2
3.23	1.8
4.10	-7.5
5.02	-19.5
6.10	-22.5
7.00	-27.0

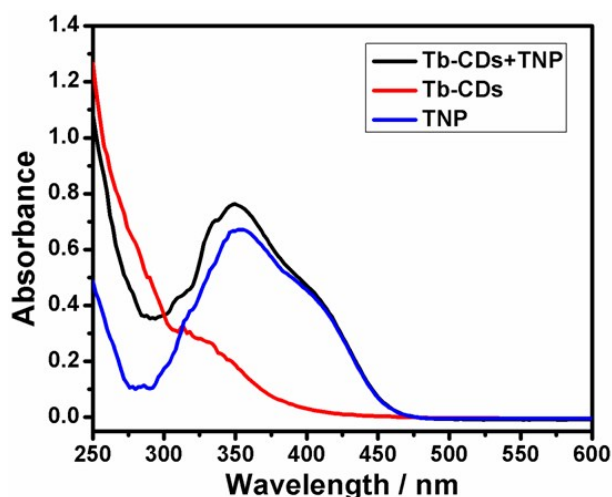


Fig.S5 The UV-Vis absorption spectra of TNP in the absence and presence of Tb-CDs.

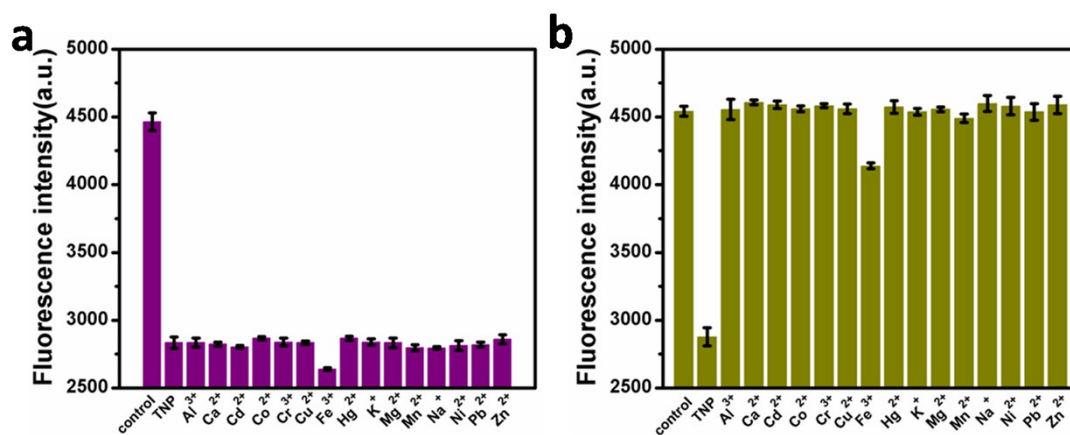


Fig.S6 Selective detection of the Tb-CDs for TNP in BR buffer (pH 7.0). Fluorescence responses of the Tb-CDs in the presence (a) and absence (b) of 75 μM TNP. The concentration of metal ions was 100 μM.

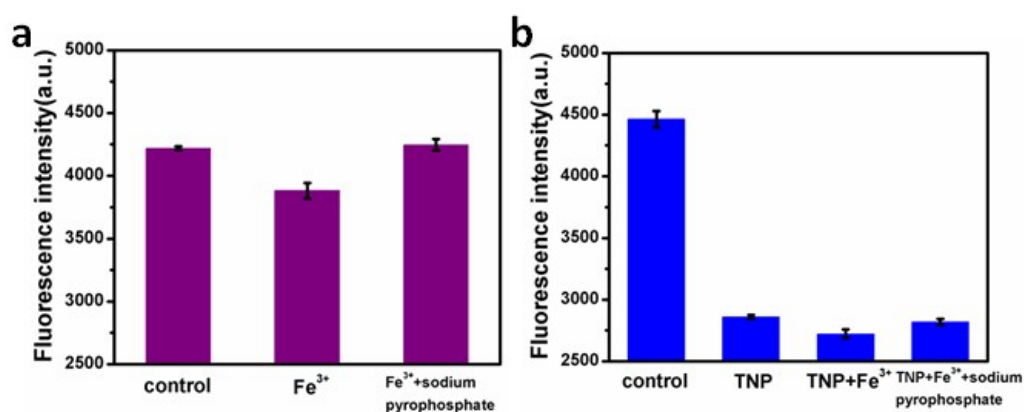
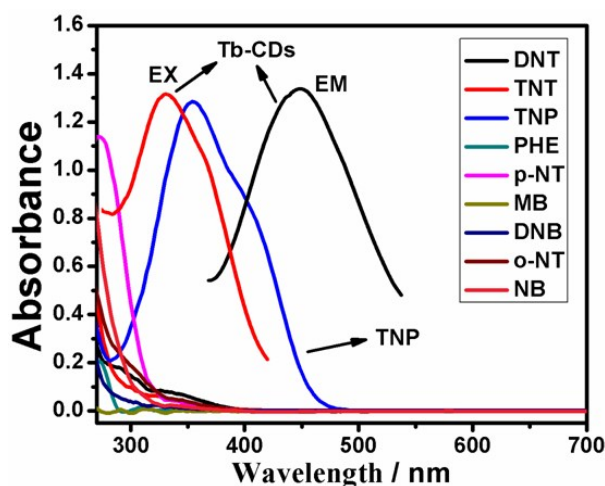
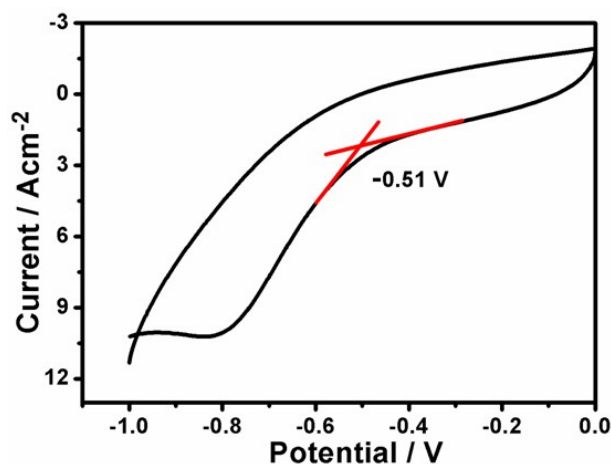


Fig.S7 Fluorescence responses of the Tb-CDs in the absence (a) and presence (b) of 75 μM TNP.  $C_{\text{Fe}^{3+}}$ , 100 μM;  $C_{\text{sodium pyrophosphate}}$ , 1 mM.



**Fig.S8** The UV-Vis absorption spectra of all nitroaromatic explosives and the fluorescence excitation and emission spectra of Tb-CDs.



**Fig.S9** Cyclic voltammograms of the Tb-CDs in the solution state. The HOMO and LUMO energy levels of Tb-CDs could be estimated according to the empirical formula:

$$E_{\text{HOMO}} = -e(E_{\text{ox}} + 4.4)$$

$$E_{\text{LUMO}} = -e(E_{\text{red}} + 4.4)$$

Where  $E_{\text{ox}}$  and  $E_{\text{red}}$  are the onset of oxidation and reduction potential for Tb-CDs, respectively. The  $E_{\text{red}}$  was determined to be -0.51 V. The corresponding  $E_{\text{LUMO}}$  was calculated to be -3.89 eV. However, the HOMO energy could not be obtained due to the irreversible of the oxidation behavior. To determine the HOMO levels, we combined the  $E_{\text{red}}$  with the optical energy band gap ( $E_{\text{g}}$ , resulting from the absorption edge in the absorption spectrum):

$$E_{\text{HOMO}} = E_{\text{LUMO}} - E_{\text{g}}^{40}$$

$E_{\text{g}}$  was estimated to be 4.42 eV. So, the  $E_{\text{HOMO}}$  was calculated to be -8.31 eV.

**Table. S2** The comparison of the determination of TNP.

Methods	Linear detection range	Detection limit	Reference
Colorimetric method with $\pi$ -stacked organic crystalline solid	/	15.2 $\mu\text{M}$	1
Fluorescent method with cadmium-pamoate metal-organic framework	0.76-11.5 ppm	$1.76 \times 10^{-8}$ g/L	2
Fluorescent method with metal-organic framework	10-400 ppm	/	3
Fluorescent method with photoluminescent carbon nanodots	0.08-100 $\mu\text{M}$	22 nM	4
Colorimetric method with Redox-Switchable Copper(I) Metallogel	/	50 $\mu\text{M}$	5
Fluorescent method with graphene quantum dots	1-60 $\mu\text{M}$	0.3 $\mu\text{M}$	6
Fluorescent method with Graphitic Carbon Nitride Nanosheets	0-0.5 $\mu\text{M}$ 0.5-10 $\mu\text{M}$	8.2 nM	7
Fluorescent method with DAP-RGO	/	125 nM	8
Fluorescent method with Tb-CDs	500nM-100 $\mu\text{M}$	0.2 $\mu\text{M}$	This work

## REFERENCES

- (1) S. Mukherjee, A. V. Desai, A. I. Inamdar, B. Manna and S. K. Ghosh, *Cryst. Growth Des.*, 2015, **15**, 3493-3497.
- (2) D. J. Ye, L. Zhao, R. F. Bogale, Y. Gao, X. Wang, X. Qian, S. Guo, P. J. Zhao and P. G. Ning, *Chem. Eur. J.*, 2015, **21**, 2029–2037.
- (3) S. R. Zhang, D. Y. Du, J. S. Qin, S. J. Bao, S. L. Li, W. W. He, Y. Q. Lan, P. Shen and Z. M. Su, *Chem. Eur. J.*, 2014, **20**, 3589–3594.
- (4) X. Deng and D. Wu, *RSC Adv.*, 2014, **4**, 42066-42070.
- (5) S. Sarkar, S. Dutta, S. Chakrabarti, P. Baire and T. Pal, *ACS Appl. Mater. interfaces*, 2014, **6**, 6308-6316.
- (6) L. Lin, M. Rong, S. Lu, X. Song, Y. Zhong, J. Yan, Y. Wang and X. Chen, *Nanoscale*, 2015, **7**, 1872-1878.
- (7) M. Rong, L. Lin, X. Song, T. Zhao, Y. Zhong, J. Yan, Y. Wang and X. Chen, *Anal. Chem.*, 2015, **87**, 1288-1296.
- (8) D. Dinda, A. Gupta, B. K. Shaw, S. Sadhu and S. K. Saha, *Appl. Mater. interfaces*, 2014, **6**, 10722-10728.